mode in the Raman for the trans complex. Only one band is observed in both the infrared and Raman spectra for both compounds. In addition, the wave numbers of the bands are almost the same in the infrared and Raman spectra although the trans bands are ~ 20 cm^{-1} above those of the cis. We think there are two reasons for this. First, although the symmetric and asymmetric bands in $PtCl_2L_2$ usually are well resolved, being up to 25 cm^{-1} apart, they may be as little as 8 cm^{-1} apart[29] and on a geometrical basis should have the same wavenumber.[30] The separation can be related to ligand field strength.[31] We suggest that for the trans compound, this difference is reduced to 4 ± 2 cm^{-1}. Second, the resolution of the bands for the cis compound is not good. The width at half-height for the infrared band is 30 cm^{-1} and for the Raman band is 13 cm^{-1}. On the assumption of a similar separation of the symmetric and asymmetric modes, 5–10 cm^{-1}, it is reasonable that no resolution of the bands has taken place. Thus, although band position allows identification of the compounds, counting numbers of bands does not, in this case, allow differentiation.

We conclude that although literature procedures for the preparation of *cis*-$PtCl_2(amine)_2$ do give the desired products, the process of recrystallization may cause cis to trans interconversion. This interconversion is clearly easier than had previously been assumed. Thus procedures for purifying *cis*-$PtCl_2(amine)_2$ complexes for animal tests should be monitored carefully to make sure that cis–trans interconversion has not taken place. Further, infrared–Raman spectroscopy is not, in itself, a completely unambiguous method of differentiating cis and trans isomers.

Acknowledgment. We acknowledge, with thanks, financial support from the National Cancer Institute of Canada, the Natural Sciences and Engineering Research Council of Canada, the McMaster University Science and Engineering Research Board, and Johnson, Matthey, Mallory Ltd.

Registry No. *cis*-$PtCl_2(C_4H_7NH_2)_2$, 38780-37-9; *trans*-$PtCl_2(C_4H_7NH_2)_2$, 76173-93-8.

Supplementary Material Available: Listings of structure factor amplitudes (10 pages). Ordering information is given on any current masthead page.

(29) Pfeffer, M.; Braunstein, P.; Dehand, J. *Spectrochim. Acta, Part A* **1974**, *30A*, 341.
(30) Colthup, N. B.; Daly, L. H.; Wiberley, S. E. "Introduction to Infrared and Raman Spectroscopy"; Academic Press: New York, 1964; p 183.
(31) Howard-Lock, H. E.; Lock, C. J. L.; Turner, G., to be submitted for publication in *Can. J. Chem.*

Contribution from the Department of Chemistry, University of Virginia, Charlottesville, Virginia 22901

Oxidation of Phenacetin and Related Amides to Their Hydroxamic Acids. Crystal Structures of the Dioxomolybdenum(VI) Hydroxamates Derived from Phenacetin and Acetanilide

GREG A. BREWER and EKK SINN*

Received September 2, 1980

An existing method of oxidation involving oxodiperoxo(hexamethylphosphoramide)molybdenum(VI) has been adapted for the direct conversion of phenacetin and related amides to their respective hydroxamic acids. The hydroxamic acids are initially isolated as their stable dioxomolybdenum(VI) salts, in which form they can conveniently be stored and from which they are readily liberated by ligand displacement. The hydroxamic acids are of interest as the suspected toxic metabolites of several related drugs. The Mo(VI) derivatives of two analgesics, phenacetin and acetanilide, have been characterized by single-crystal X-ray diffraction. The ligand environment about the Mo atom is a markedly distorted octahedron in each case, with the dioxo O atoms bonded cis to each other, while trans to these bonds the hydroxamate Mo–O bonds are elongated. There is no conjugation between the phenyl rings and the hydroxamic acid group. Crystal data: MoO_2L_2, space group $P2_1/c$, $Z = 4$, $a = 12.350$ (6) Å, $b = 17.477$ (3) Å, $c = 10.309$ (7) Å, $\beta = 95.25$ (3) °, $V = 2216$ Å^3, $R = 5.0\%$, 2738 reflections; $MoO_2L'_2$, space group *Pbca*, $Z = 8$, $a = 13.137$ (3) Å, $b = 11.620$ (3) Å, $c = 22.820$ (5) Å, $V = 3483$ Å^3, $R = 4.7\%$, 1549 reflections. L and L′ represent the hydroxamate anions derived from phenacetin and acetanilide, respectively.

Introduction

The oxidation of amides to the corresponding hydroxamic acids is a recognized pathway for the metabolism of certain *N*-acyl aromatic amines.[1] Phenacetin, Figure 1, a widely used analgesic and antipyretic, is metabolized in the liver, a major route being deethylation to acetaldehyde and acetaminophen.[2] Similarly, the metabolism of acetanilide involves rapid hydroxylation to acetaminophen, through which the analgesic and antipyretic effects are chiefly exerted.[2] N-Oxidation of phenacetin has been proposed to account for the appearance of hydroquinone and acetamide as minor urinary metabolites of this drug.[3] Further, the N-hydroxylation of phenacetin has been suggested to be the cause of acute nephrotoxicity of this molecule and related derivatives.[4]

The relationship between large doses and renal failure in man is widely accepted although the exact mechanism of this process has not been determined.[5] It has been shown that there is a correlation between the toxicity of phenacetin and related derivatives and pretreatment with compounds known to stimulate the cytochrome P-450 mixed-oxidase system.[6] This also suggests that amide oxidation products may be key intermediates in the toxic pathways open to phenacetin and related molecules.

The testing of the postulate that the hydroxamic acids are the toxic intermediates is greatly hampered by the lack of a ready supply of these acids. The syntheses are difficult, and storage presents further problems, due to rapid decomposition.

(1) Irving, C. C. "Metabolic Conjugation and Metabolic Hydrolysis"; Academic Press: New York, 1970; Vol. 1, p 53.
(2) Clarke, E. G. C. "Isolation and Identification of Drugs"; Pharmaceutical Press: London, 1974.
(3) Nery, R. *Biochem. J.* **1971**, *122*, 317.
(4) Calder, P.; Creek, M.; Williams, P. *J. Med. Chem.* **1973**, *16*, 1523.
(5) Harvold, R. *Am. J. Med.* **1969**, *35*, 481.
(6) Potter, W. S.; Thargierson, S. S.; Jeller, D. J.; Mitchell, J. R. Pharmacology **1974**, *12*, 129.

0020-1669/81/1320-1823$01.25/0

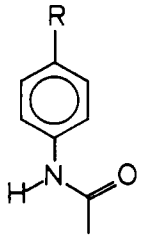

Figure 1. Acetalide derivatives: R = H, acetanilide; R = OH, acetaminophen; R = OC_2H_5, phenacetin.

Considering the biological significance of amide oxidation, there have been relatively few procedures developed for the in vitro process.[7] Animal studies done on *N*-hydroxy-*p*-acetophenatidine, to clarify its role in the nephrotoxic effects of phenacetin, were carried out with samples prepared from an indirect source (vide infra), as opposed to the amide itself.[4] In general it would be advantageous to produce the hydroxamic acid to be studied directly from the parent amide, thus eliminating costly synthetic steps.

An unmodified literature method for amide oxidation[8] was found not to work and shown to be in conflict with thermodynamic requirements. A modified procedure works and is described here. The amides are oxidized directly by oxodiperoxo(hexamethylphosphoramide)molybdenum(VI) (MoO_5HMPT)[9] to their corresponding hydroxamates, which are isolated as the highly stable *cis*-dioxomolybdenum(VI) complexes. Treatment with EDTA readily releases hydroxamic acid, the alleged toxic intermediate. The generality of the reaction was demonstrated by the oxidation of several analogues, also reported here. Two of the products were characterized crystallographically as their dioxomolybdenum complexes. Apart from such molybdenum complexes with ligands of biological significance, the importance of molydenum(V) and -(VI) in a number of enzymic systems makes its coordination geometry of particular interest.[10-13]

Experimental Section

Preparation of the Complexes. Bis(trimethylsilyl)acetamide[14] (1.15 g, 5.58 mmol) was injected into a flask under nitrogen atmosphere containing phenacetin (1 g, 5.58 mmol). The slurry was heated at 40 °C for 5 min, as previously described,[15] and then diluted with 10 mL of dichloromethane. A solution of oxodiperoxo(hexamethylphosphoramide)molybdenum(VI) (MoO_5HMPT) (0.988 g, 7.799 mmol) in dichloromethane (20 mL) was injected into the reaction vessel, and the mixture was stirred at room temperature overnight. Evaporation of the solvent yielded the crude hydroxamate, which was crystallized from chloroform (0.87 g, mp 179–180 °C, 60%).

The same procedure was used to produce the molybdenum complexes of the following amides: acetanilide, *p*-chloroacetanilide, *p*-benzoyloxyacetanilide, and benzanilide. In each case a pale yellow complex resulted.

The NMR and IR spectra were obtained on Varian T-60 and Perkin-Elmer 337 grating spectrometers, respectively.

Crystal Data for MoO_2L_2: $MoO_8N_2C_{20}H_{24}$, mol wt 516, space group $P2_1/c$, $Z = 4$, $a = 12.350$ (6) Å, $b = 17.477$ (3) Å, $c = 10.309$ (7) Å, $\beta = 95.25$ (3)°, $V = 2216$ Å^3, $\rho_{calcd} = 1.55$ g cm^{-3}, $\rho_{obsd} = 1.53$ g cm^{-3}, μ(Mo Kα) = 6.3 cm^{-1}; crystal dimensions (distances in mm of faces from centroid) (100)0.16, ($\bar{1}$00) 0.16, (010) 0.13, (0$\bar{1}$0) 0.13, (001) 0.10, (00$\bar{1}$) 0.10; maximum, minimum transmission coefficients 0.94, 0.92.

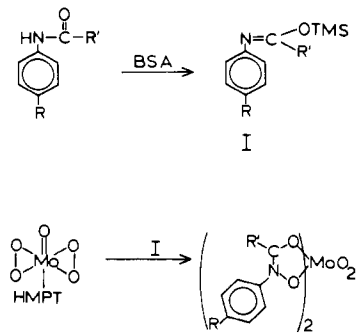

Figure 2. Generalized reaction scheme (HMPT = hexamethylphosphoramide).

Crystal Data for $MoO_2L'_2$: $MoO_6N_2C_{16}H_{16}$, mol wt 428, space group *Pbca*, $Z = 8$, $a = 13.137$ (3) Å, $b = 11.620$ (3) Å, $c = 22.820$ (5) Å, $V = 3483$ Å^3, $\rho_{calcd} = 1.63$ g cm^{-3}, $\rho_{obsd} = 1.59$ g cm^{-3}, μ(Mo Kα) = 7.4 cm^{-1}; crystal dimensions (mm from centroid) (010) 0.32, (0$\bar{1}$0) 0.32, (101) 0.06, ($\bar{1}$0$\bar{1}$) 0.06, (10$\bar{1}$) 0.06, ($\bar{1}$01) 0.06; maximum, minimum transmission coefficients 0.97, 0.95.

Cell dimensions and space group data were obtained by standard methods on an Enraf-Nonius four-circle CAD-4 diffractometer. The θ–2θ scan technique was used, as previously described,[16] to record the intensities for all nonequivalent reflections for which $1.5° < 2\theta < 50°$ for MoO_2L_2 and $1.5° < 2\theta < 48°$ for $MoO_2L'_2$. Scan widths were calculated as $(A + B \tan \theta)°$, where A is estimated from the mosaicity of the crystal and B allows for the increase in width of peak due to Kα_1–Kα_2 splitting. The values of A and B were 0.60 and 0.35°, respectively, for both complexes.

The intensities of four standard reflections, monitored for each crystal at 100-reflection intervals, showed no greater fluctuation than those expected from Poisson statistics. The raw intensity data were corrected for Lorentz–polarization effects and absorption. Of the 3345 independent intensities for MoO_2L_2 and 2689 for $MoO_2L'_2$, there were 2738 and 1549, respectively, with $F_o^2 > 3\sigma(F_o^2)$, where $\sigma(F_o^2)$ was estimated from counting statistics.[17] These data were used in the final refinement of the structural parameters.

Structure Determinations. The positions of the molybdenum atom and one ligand atom were determined for both MoO_2L_2 and $MoO_2L'_2$ from three-dimensional Patterson syntheses calculated from all intensity data. For each crystal, the intensity data were phased sufficiently well by these positional coordinates to permit location of the remaining nonhydrogen atoms from Fourier difference functions. Full-matrix least-squares refinement was carried out as previously described.[16] Anisotropic temperature factors were then introduced for all nonhydrogen atoms. Further Fourier difference functions permitted location of the hydrogen atoms, which were included in the refinement for three cycles of least squares and then held fixed. The models converged with $R = 5.0$, $R_w = 5.9\%$ for MoO_2L_2 and $R = 4.7$, $R_w = 5.2\%$ for $MoO_2L'_2$. Final Fourier difference functions were featureless. Tables of the observed and calculated structure factors are available.[18] The principal programs used are as previously described.[16]

Results and Discussion

Reactions. The reaction scheme is given in Figure 2. The hydroxamic acids are initially isolated as their pale yellow dioxomolybdenum(VI) salts, from which they are readily liberated by ligand displacement, as shown. These molybdenum complexes are stable and convenient to handle and provide a ready means of storage for the acids. The difference between this method and that suggested by Matlin and Sammes[8] is in the method of silylation of the amide. Attempts

(7) Black, D. S.; Brown, R. F. C.; Wade, A. M. *Tetrahedron Lett.* **1971**, 4519.
(8) Matlin, S.; Sammes, P. *J. Chem. Soc., Chem. Commun.* **1972**, 1222.
(9) LeCarpentier, P. J.-M.; Schlupp, R.; Weiss, R. *Acta Crystallogr., Sect. B* **1972**, *B28*, 1278.
(10) Butcher, R. J.; Penfold, B. R.; Sinn, E. *J. Chem. Soc., Dalton Trans.* **1979**, 668.
(11) Bray, R. C.; Swann, J. C. *Struct. Bonding (Berlin)* **1972**, *11*, 107.
(12) Wentworth, R. A. D. *Coord. Chem. Rev.* **1976**, *18*, 1.
(13) Butcher, R. J.; Powell, H. K. J.; Wilkins, C. J.; Young, S. H. *J. Chem. Soc., Dalton Trans.* **1976**, 356.
(14) Birkafer, L.; Ritter, A. *Newer Methods Prep. Org. Chem.* **1968**, *5*, 211.
(15) Klebe, J. F.; Finkheimer, H.; White, D. M. *J. Am. Chem. Soc.* **1966**, *88*, 3390.
(16) Freyberg, D. P.; Mockler, G. M.; Sinn, E. *J. Chem. Soc., Dalton Trans.* **1976**, 447.
(17) Corfield, P. W. R.; Doedens, R. J.; Ibers, J. A. *Inorg. Chem.* **1967**, *6*, 197.
(18) Supplementary material.

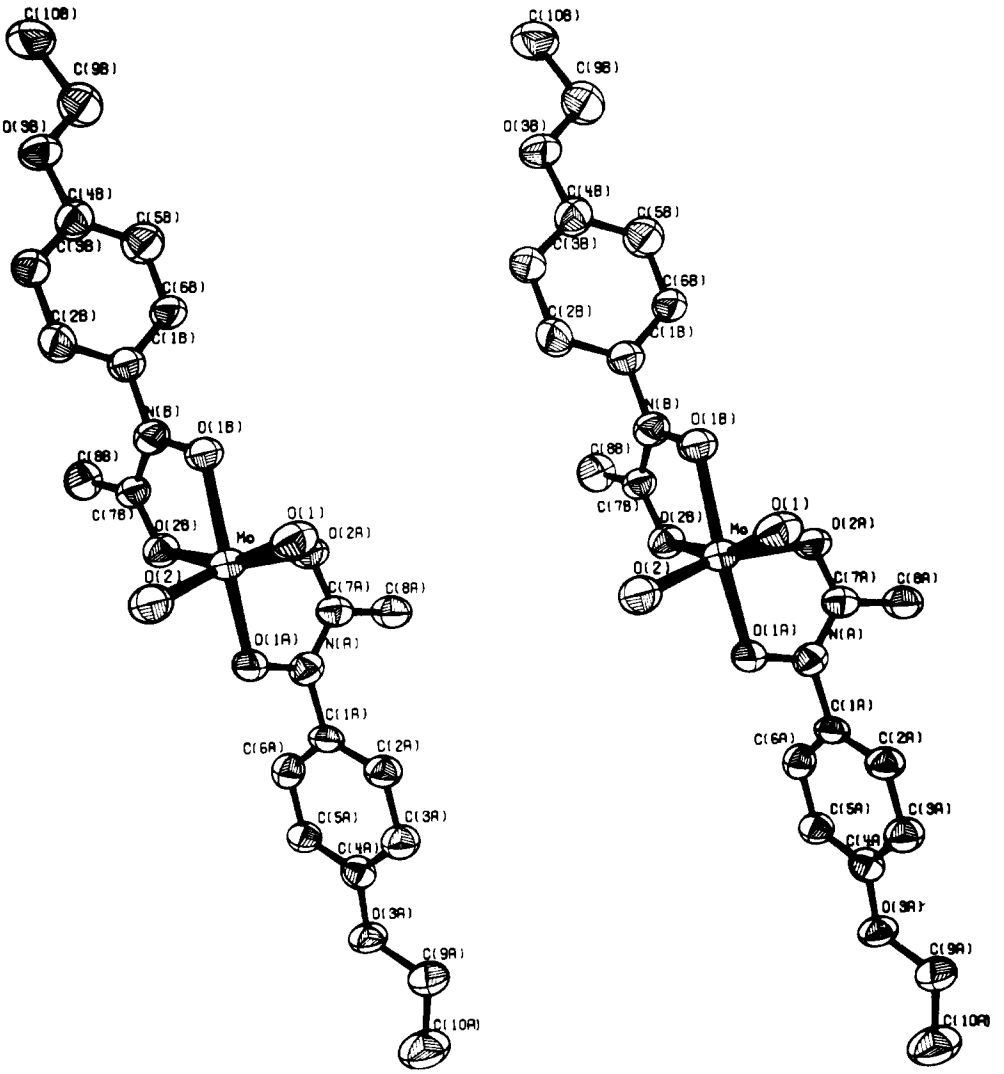

Figure 3. Stereoview of the MoO_2L_2 molecule, the complex of the phenacetin metabolite.

on our part to duplicate the silylation of acetanilide with hexamethyldisilizane (HMDS) as directed by Matlin and Sammes proved unsuccessful. Even prolonged heating of the amide with HMDS and a sulfuric acid catalyst failed to yield any detectable quantity of silylated amide. There is a thermodynamic reason why this should not work: it has been shown that silyl proton exchange is an equilibrium process[15] and that the position of this equilibrium depends on the strength of the silyl donor. Thus, a weak silyl donor, such as HMDS, cannot be used to silylate a reluctant acceptor, such as amides. The silylations done in this work were carried out with bis(trimethylsilyl)acetamide, an extremely powerful silyl donor.

There is an organic method of synthesis for hydroxamic acids. The key steps in this method involve the acetylation[19] of a phenylhydroxylamine available from the reduction of nitro aromatics with zinc.[20] Although not particularly long, this approach suffers from serious drawbacks. The exact conditions of the reduction of nitro aromatics are critical to the yield. The reaction works well for nitrobenzene, but problems generally develop for substituted derivatives. The hydroxylamine produced is generally unstable if not treated properly. The acetylation step can cause problems also: diacetyl derivatives are possible contaminants, as are rearrangement products arising from traces of acid in the reaction conditions. These problems lead to troublesome mixtures which may be separated by column chromatography.[21]

The present method is free from many of the above problems. The transformation from amide to hydroxamate takes place in one vessel, the first step being quantitative. The hydroxamate is the only product isolated from the reaction medium, being fairly free of impurities. Also, as the dioxo species it is stable and may be stored indefinitely for future use.

Crystal Structures. Final positional and thermal parameters for MoO_2L_2 and $MoO_2L'_2$ are given in Table I. Tables II and III contain the bond lengths and angles. The digits in parentheses in the tables are the estimated standard deviations in the least significant figures quoted and were derived from the inverse matrix in the course of least-squares refinement calculations. Figure 3 is a stereoview of MoO_2L_2, the complex of the phenacetin metabolite. Figure 4 shows the packing in the unit cell. Figure 5 is a stereoview of $MoO_2L'_2$, the metabolite of acetanilide. The atom names are analogous to that of Figure 3. Figure 6 is the packing diagram of $MoO_2L'_2$.

Each of the complexes crystallizes as individual neutral molecules, with the closest intermolecular contacts in MoO_2L_2 being between the monodentate oxygen ligands and the acetyl carbon of the next molecule (O(2)–C(7A) = 2.944 (4) Å,

(19) Smissman, E.; Corbett, M. *J. Org. Chem.* **1972**, *37*, 1847.
(20) Kamm, G. "Organic Syntheses"; Wiley: New York, 1941; Vol. 1, p 445.
(21) Gemborys, M.; Gribble, G. *J. Med. Chem.* **1978**, *21*, 649.

Table I. Positional and Thermal Parameters and Their Estimated Standard Deviations[a]

(a) $MoO_2(O_3NC_{10}H_{12})_2$

atom	x	y	z	B_{11}	B_{22}	B_{33}	B_{12}	B_{13}	B_{23}
Mo	−0.08881 (3)	0.21412 (2)	0.09701 (4)	2.33 (1)	3.24 (2)	3.44 (2)	−0.01 (1)	0.56 (1)	0.00 (2)
O(1)	−0.1223 (3)	0.2857 (2)	−0.0113 (3)	3.5 (1)	4.4 (2)	5.2 (2)	0.2 (1)	1.3 (1)	1.1 (1)
O(2)	−0.0221 (3)	0.2598 (2)	0.2267 (3)	3.7 (1)	4.4 (2)	4.4 (2)	−0.4 (1)	0.8 (1)	−0.9 (1)
O(1A)	0.0571 (2)	0.1719 (2)	0.0568 (3)	2.3 (1)	4.7 (2)	3.4 (1)	0.3 (1)	0.2 (1)	−0.7 (1)
O(2A)	−0.1213 (2)	0.1289 (2)	−0.0586 (3)	2.5 (1)	4.3 (2)	4.0 (1)	−0.3 (1)	0.6 (1)	−0.6 (1)
O(3A)	0.4807 (3)	0.0705 (2)	−0.1687 (3)	2.6 (1)	5.3 (2)	4.8 (2)	0.8 (1)	0.9 (1)	0.9 (1)
O(1B)	−0.2467 (2)	0.2108 (2)	0.1341 (3)	2.4 (1)	3.9 (1)	3.7 (1)	0.3 (1)	0.6 (1)	0.8 (1)
O(2B)	−0.1084 (2)	0.1119 (2)	0.2157 (3)	3.0 (1)	3.4 (1)	3.8 (1)	0.6 (1)	0.6 (1)	0.3 (1)
O(3B)	−0.6795 (3)	0.1767 (2)	0.4164 (3)	2.9 (1)	5.7 (2)	4.7 (2)	−0.2 (1)	1.0 (1)	−0.6 (2)
N(A)	0.0573 (3)	0.1235 (2)	−0.0504 (4)	2.6 (1)	3.7 (2)	3.5 (2)	0.2 (1)	0.7 (1)	−0.2 (1)
N(B)	−0.2736 (3)	0.1589 (2)	0.2277 (4)	2.7 (2)	3.8 (2)	3.5 (2)	−0.2 (1)	0.7 (1)	0.5 (1)
C(1A)	0.1647 (4)	0.1079 (3)	−0.0878 (4)	2.5 (2)	3.5 (2)	3.4 (2)	0.2 (2)	0.2 (2)	−0.4 (2)
C(2A)	0.2042 (4)	0.1502 (3)	−0.1842 (5)	2.6 (2)	3.9 (2)	4.1 (2)	0.7 (2)	0.4 (2)	0.8 (2)
C(3A)	0.3102 (4)	0.1384 (3)	−0.2180 (5)	3.2 (2)	4.0 (2)	4.2 (2)	0.3 (2)	0.6 (2)	0.8 (2)
C(4A)	0.3758 (4)	0.0843 (3)	−0.1491 (5)	2.8 (2)	3.4 (2)	3.7 (2)	0.2 (2)	0.2 (2)	−0.1 (2)
C(5A)	0.3339 (4)	0.0413 (3)	−0.0526 (5)	3.1 (2)	4.1 (2)	3.8 (2)	1.0 (2)	0.3 (2)	0.5 (2)
C(6A)	0.2275 (4)	0.0522 (3)	−0.0213 (4)	3.4 (2)	3.7 (2)	3.4 (2)	0.0 (2)	0.5 (2)	0.2 (2)
C(7A)	−0.0373 (4)	0.1042 (3)	−0.1074 (5)	2.9 (2)	3.2 (2)	4.0 (2)	−0.1 (2)	0.6 (2)	0.2 (2)
C(8A)	−0.0458 (4)	0.0545 (3)	−0.2252 (5)	3.3 (2)	4.8 (2)	4.4 (2)	0.0 (2)	0.6 (2)	−0.9 (2)
C(9A)	0.5272 (4)	0.1101 (3)	−0.2735 (5)	3.2 (2)	5.8 (3)	4.9 (2)	0.1 (2)	1.1 (2)	0.2 (2)
C(10A)	0.6450 (5)	0.0886 (4)	−0.2700 (7)	4.3 (3)	7.8 (4)	9.1 (4)	1.5 (3)	2.3 (3)	2.2 (3)
C(1B)	−0.3791 (4)	0.1673 (3)	0.2702 (4)	2.9 (2)	3.4 (2)	3.4 (2)	0.1 (2)	0.5 (2)	0.2 (2)
C(2B)	−0.3926 (4)	0.2041 (3)	0.3861 (5)	2.8 (2)	4.5 (2)	3.5 (2)	−0.8 (2)	0.1 (2)	−0.2 (2)
C(3B)	−0.4953 (4)	0.2076 (3)	0.4306 (5)	3.4 (2)	4.6 (2)	3.5 (2)	−0.4 (2)	0.5 (2)	−0.7 (2)
C(4B)	−0.5838 (4)	0.1740 (3)	0.3596 (5)	3.1 (2)	3.8 (2)	3.6 (2)	0.1 (2)	0.8 (2)	0.2 (2)
C(5B)	−0.5724 (4)	0.1418 (3)	0.2401 (5)	3.0 (2)	5.8 (3)	5.0 (2)	−0.7 (2)	0.4 (2)	−1.4 (2)
C(6B)	−0.4694 (4)	0.1386 (3)	0.1954 (5)	3.1 (2)	5.1 (2)	3.6 (2)	−0.3 (2)	0.4 (2)	−1.3 (2)
C(7B)	−0.1977 (4)	0.1085 (3)	0.2654 (4)	3.0 (2)	3.1 (2)	3.3 (2)	−0.2 (2)	0.5 (2)	−0.0 (2)
C(8B)	−0.2176 (4)	0.0498 (3)	0.3653 (5)	4.4 (2)	4.0 (2)	4.0 (2)	0.2 (2)	0.6 (2)	0.9 (2)
C(9B)	−0.7728 (4)	0.1404 (4)	0.3502 (6)	3.3 (2)	5.7 (3)	5.4 (3)	−0.7 (2)	0.3 (2)	−0.9 (2)
C(10B)	−0.8635 (5)	0.1440 (4)	0.4361 (6)	3.1 (2)	6.4 (3)	6.0 (3)	0.2 (2)	0.7 (2)	0.3 (3)

atom	x	y	z	B, Å^2	atom	x	y	z	B, Å^2
H(2A)	0.150 (5)	0.179 (3)	−0.237 (5)	4 (1)	H(2B)	−0.323 (5)	0.221 (3)	0.429 (6)	4 (1)
H(3A)	0.333 (5)	0.163 (3)	−0.297 (5)	4 (1)	H(3B)	−0.503 (5)	0.229 (3)	0.524 (5)	3 (1)
H(5A)	0.369 (5)	0.005 (4)	−0.009 (5)	4 (1)	H(5B)	−0.641 (5)	0.120 (3)	0.189 (6)	4 (1)
H(6A)	0.188 (4)	0.020 (3)	0.055 (5)	3 (1)	H(6B)	−0.479 (5)	0.116 (3)	0.115 (5)	4 (1)
H(8A1)	−0.001 (5)	0.017 (3)	−0.207 (5)	4 (1)	H(8B1)	−0.295 (6)	0.048 (4)	0.371 (6)	6 (2)
H(8A2)	−0.120 (5)	0.043 (4)	−0.269 (6)	5 (2)	H(8B2)	−0.171 (5)	0.053 (3)	0.444 (5)	4 (1)
H(8A3)	−0.019 (5)	0.075 (4)	−0.293 (6)	6 (2)	H(8B2)	−0.175 (5)	0.002 (4)	0.318 (6)	4 (1)
H(9A1)	0.518 (4)	0.162 (3)	−0.249 (5)	3 (1)	H(9B1)	−0.795 (5)	0.166 (4)	0.255 (5)	5 (2)
H(9A2)	0.500 (4)	0.091 (3)	−0.337 (5)	3 (1)	H(9B2)	−0.784 (5)	0.087 (4)	0.316 (6)	5 (2)
H(10A1)	0.664 (5)	0.109 (4)	−0.208 (5)	5 (1)	H(10B1)	−0.837 (5)	0.112 (3)	0.497 (5)	4 (1)
H(10A2)	0.669 (5)	0.125 (3)	−0.334 (5)	4 (1)	H(10B2)	−0.852 (6)	0.188 (4)	0.469 (7)	6 (2)
H(10A3)	0.662 (6)	0.034 (4)	−0.282 (6)	6 (2)	H(10B3)	−0.929 (5)	0.120 (4)	0.401 (6)	6 (2)

(b) $MoO_2(O_2NC_8H_8)_2$

atom	x	y	z	B_{11}	B_{22}	B_{33}	B_{12}	B_{13}	B_{23}
Mo	0.24659 (4)	0.11905 (4)	−0.09612 (2)	3.26 (2)	3.58 (2)	3.05 (2)	0.26 (3)	0.07 (2)	0.24 (2)
O(1)	0.2882 (4)	0.0113 (4)	−0.1407 (2)	5.0 (2)	5.7 (3)	5.0 (2)	1.7 (2)	−0.2 (2)	−0.9 (2)
O(2)	0.3422 (4)	0.2166 (4)	−0.0951 (2)	5.3 (2)	5.7 (3)	5.0 (2)	−1.2 (2)	0.6 (2)	1.2 (2)
O(1A)	0.2908 (3)	0.0745 (4)	−0.0142 (2)	4.2 (2)	4.2 (2)	3.7 (2)	−0.8 (2)	−0.8 (2)	1.2 (2)
O(2A)	0.1293 (3)	0.0033 (4)	−0.0611 (2)	3.5 (2)	3.8 (2)	4.4 (2)	−0.4 (2)	−0.2 (2)	0.4 (2)
O(1B)	0.1492 (3)	0.1655 (4)	−0.1598 (2)	4.6 (2)	4.3 (2)	3.0 (2)	1.4 (2)	−0.3 (2)	−0.3 (2)
O(2B)	0.1426 (3)	0.2480 (4)	−0.0580 (2)	4.6 (2)	3.4 (2)	3.5 (2)	0.8 (2)	−0.6 (2)	−0.1 (2)
N(A)	0.2348 (4)	−0.0105 (4)	0.0135 (2)	3.8 (3)	3.5 (2)	3.9 (2)	−0.7 (2)	0.6 (2)	0.4 (2)
N(B)	0.0833 (4)	0.2560 (4)	−0.1478 (2)	3.8 (2)	3.5 (2)	3.4 (2)	1.0 (2)	−0.2 (2)	−0.2 (2)
C(1A)	0.2729 (5)	−0.0431 (5)	0.0698 (3)	4.8 (3)	3.5 (3)	3.1 (3)	−0.3 (3)	0.4 (3)	0.8 (2)
C(2A)	0.2439 (6)	0.0177 (7)	0.1189 (4)	5.7 (4)	5.5 (4)	5.6 (4)	0.2 (4)	1.0 (4)	−1.5 (3)
C(3A)	0.2808 (7)	−0.0135 (8)	0.1730 (3)	8.5 (5)	8.2 (5)	3.8 (3)	−1.8 (4)	0.9 (4)	−1.8 (4)
C(4A)	0.3497 (7)	−0.1014 (7)	0.1783 (3)	8.9 (5)	7.1 (5)	3.4 (3)	−2.3 (4)	−1.2 (4)	1.1 (3)
C(5A)	0.3795 (7)	−0.1607 (7)	0.1288 (4)	8.2 (5)	4.9 (4)	6.7 (5)	0.1 (4)	−2.0 (4)	1.5 (4)
C(6A)	0.3398 (7)	−0.1331 (6)	0.0753 (3)	7.8 (5)	4.1 (4)	3.5 (3)	1.0 (4)	−0.1 (3)	0.3 (3)
C(7A)	0.1511 (5)	−0.0437 (5)	−0.0128 (3)	3.7 (3)	3.1 (3)	3.8 (3)	−0.3 (3)	0.5 (3)	−0.0 (3)
C(8A)	0.0856 (6)	−0.1344 (6)	0.0135 (4)	4.9 (4)	4.8 (4)	6.2 (4)	−0.8 (3)	1.2 (3)	0.7 (3)
C(1B)	0.0209 (5)	0.2911 (5)	−0.1969 (3)	4.0 (3)	3.2 (3)	3.6 (3)	0.4 (3)	−0.7 (3)	−0.6 (3)
C(2B)	0.0524 (6)	0.3805 (6)	−0.2316 (3)	5.3 (4)	4.5 (3)	4.0 (3)	−1.5 (3)	−0.5 (3)	0.5 (3)
C(3B)	−0.0081 (7)	0.4084 (6)	−0.2803 (3)	8.9 (5)	4.2 (3)	4.3 (3)	−0.4 (4)	−1.3 (4)	0.7 (3)
C(4B)	−0.0940 (6)	0.3513 (6)	−0.2918 (3)	7.5 (4)	5.3 (4)	3.3 (3)	1.8 (4)	−2.1 (3)	−0.7 (3)
C(5B)	−0.1247 (6)	0.2612 (6)	−0.2565 (3)	5.8 (4)	5.3 (4)	4.9 (4)	−0.5 (4)	−2.3 (3)	−0.2 (3)
C(6B)	−0.0663 (6)	0.2318 (6)	−0.2080 (3)	5.4 (4)	3.8 (3)	5.1 (4)	−0.3 (3)	−1.0 (3)	0.2 (3)
C(7B)	0.0826 (5)	0.2951 (5)	−0.0941 (3)	3.5 (3)	3.1 (3)	3.2 (3)	−0.2 (2)	0.3 (3)	0.1 (3)
C(8B)	0.0141 (5)	0.3908 (6)	−0.0774 (3)	4.3 (3)	3.6 (3)	4.7 (3)	0.6 (3)	0.8 (3)	−0.8 (3)

Table I (*Continued*)

atom	x	y	z	B, Å²	atom	x	y	z	B, Å²
H(2A)	0.197 (5)	0.083 (5)	0.113 (3)	5 (2)	H(5B)	−0.190 (5)	0.215 (5)	−0.264 (3)	6 (2)
H(3A)	0.258 (4)	0.025 (5)	0.205 (3)	5 (2)	H(6B)	−0.087 (4)	0.170 (5)	−0.184 (3)	5 (1)
H(4A)	0.371 (5)	−0.126 (5)	0.219 (3)	6 (2)	H(8A1)	0.116 (5)	−0.184 (5)	0.008 (3)	6 (2)
H(5A)	0.430 (5)	−0.215 (5)	0.136 (3)	6 (2)	H(8A2)	0.006 (6)	−0.139 (5)	0.006 (3)	8 (2)
H(6A)	0.365 (5)	−0.174 (5)	0.041 (3)	5 (2)	H(8A3)	0.071 (5)	−0.119 (5)	0.054 (3)	6 (2)
H(2B)	0.110 (4)	0.416 (5)	−0.222 (2)	5 (2)	H(8B1)	−0.003 (5)	0.397 (5)	−0.048 (3)	5 (2)
H(3B)	0.011 (4)	0.469 (5)	−0.305 (3)	5 (2)	H(8B2)	−0.053 (5)	0.382 (5)	−0.086 (3)	7 (2)
H(4B)	−0.135 (5)	0.373 (5)	−0.323 (3)	6 (2)	H(8B3)	0.036 (5)	0.464 (6)	−0.083 (3)	8 (2)

[a] The form of the anisotropic thermal parameter is $\exp[-(B_{11}a^2h^2 + B_{22}b^2k^2 + B_{33}c^2l^2)/4 + (B_{12}abhk + B_{13}achl + B_{23}bckl)/2]$.

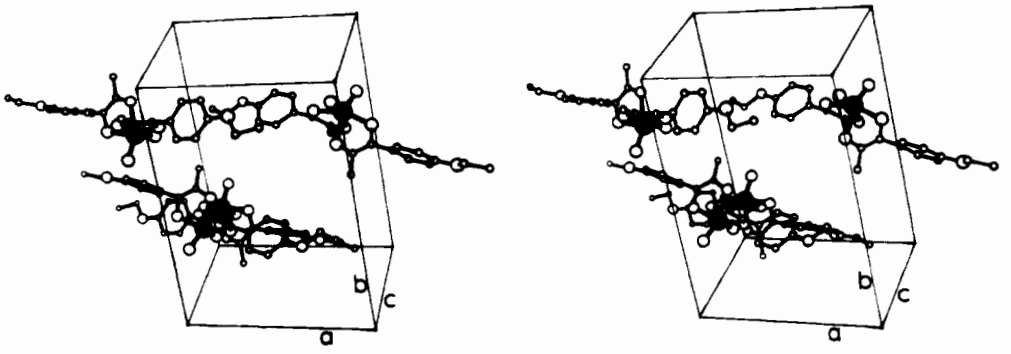

Figure 4. Molecular packing in the unit cell of MoO_2L_2.

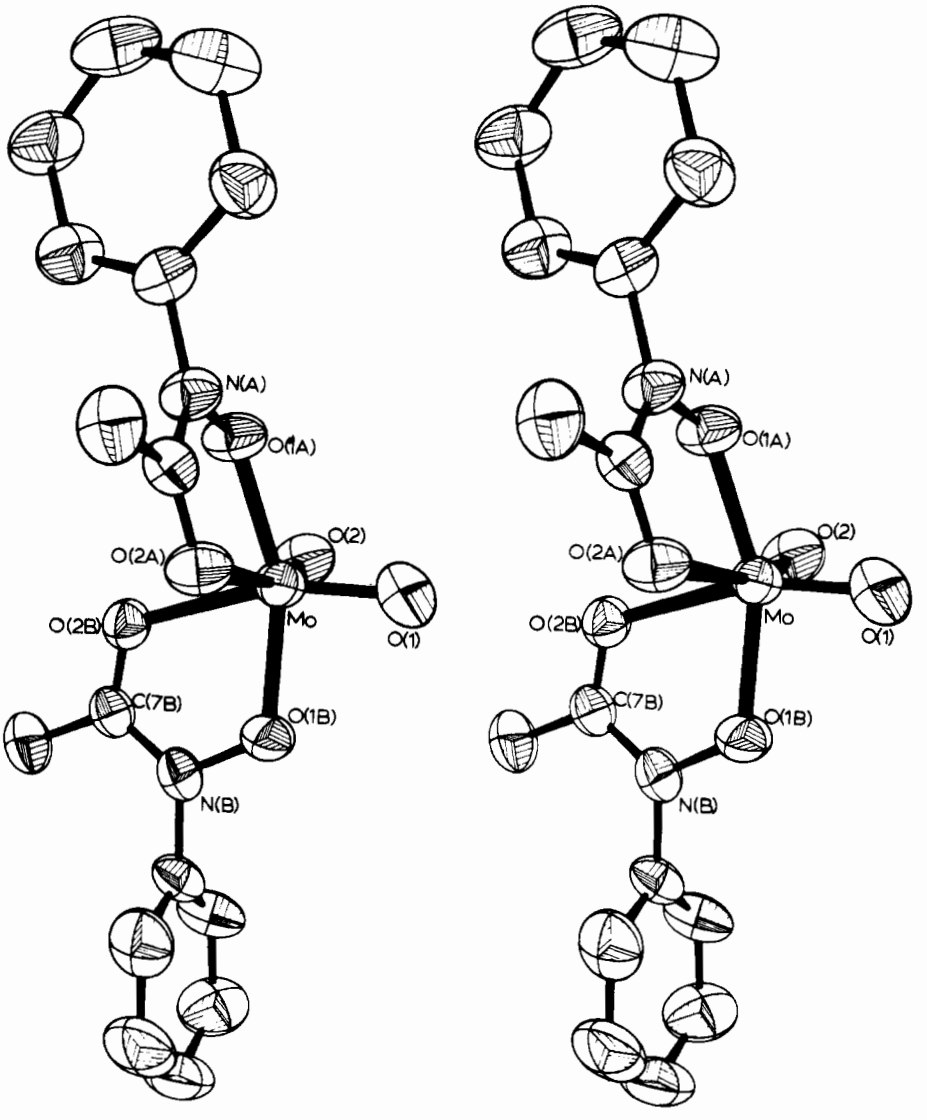

Figure 5. Stereoview of the $MoO_2L'_2$ molecule, the complex of the acetanilide metabolite.

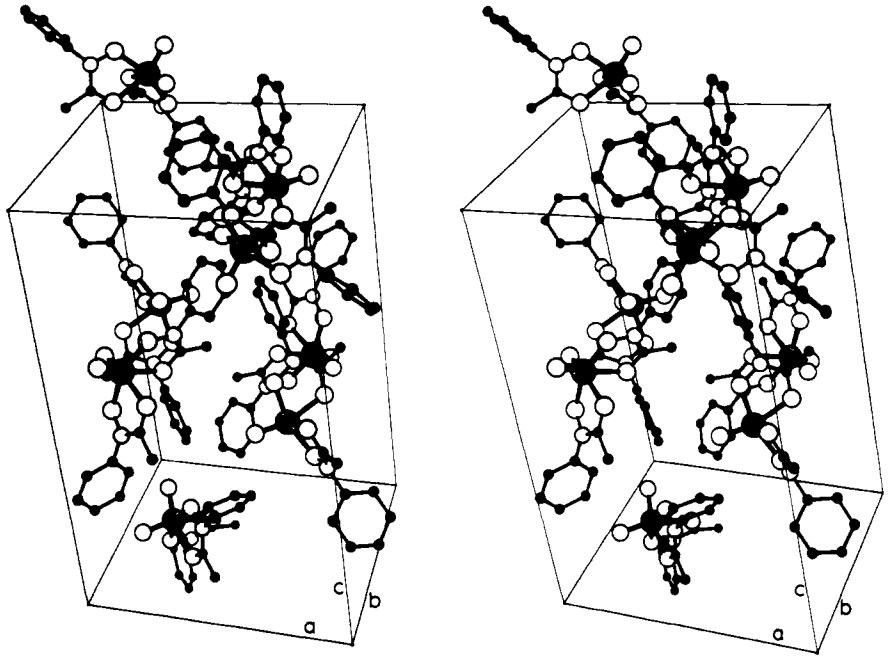

Figure 6. Molecular packing in the unit cell of $MoO_2L'_2$.

O(1)–C(7B) = 3.032 (4) Å), while in the other complex, $MoO_2L'_2$, the nearest contact is between a phenyl ring carbon atom and a monodentate oxygen of adjacent molecules (O(2)–C(4B) = 3.133 (6) Å).

Although the two complexes crystallize in different space groups and pack differently, the molybdenum environment and some features of the ligand geometry are quite similar in the two complexes. In each case, the environment about the Mo atom is a markedly distorted octahedron. The three equatorial planes of four donor atoms are approximately orthogonal (89.0, 89.7, and 89.4° in MoO_2L_2 and 89.6, 88.8, and 89.9° in $MoO_2L'_2$), but the plane which includes both the oxo oxygen atoms suffers considerable out-of-plane distortion in each complex, while essentially passing through the metal atom. The other two groups (O(1), O(1A), O(1B), O(2B) and O(2), O(1A), O(2A), O(1B)) are more closely planar but are about 0.24 Å from the metal atom in each complex. The distortion from regular octahedral geometry is further indicated by the deviation from 90° of the angles subtended at Mo by adjacent (cis) donor atoms and the deviation from 180° for trans donor atoms. For cis donors, the angles range from 73.2 to 107.5° in MoO_2L_2 and from 73.1 to 107.6° in $MoO_2L'_2$. The values for trans donors fall within 156.9–158.9 and 156.7–159.0° in MoO_2L_2 and $MoO_2L'_2$, respectively. The angle subtended by the two cis oxo O atoms is 103.9 and 105.2° for the two compounds, respectively. The deviation from the 90° expected of regular geometry is presumably due to the ligand charge repulsion. The Mo=O bonds are drastically shortened (average 1.703 and 1.698 Å in MoO_2L_2 and $MoO_2L'_2$, respectively) when compared with the other metal–ligand bonds. The bonds opposite these short vectors are somewhat elongated (average 2.195, 2.200 Å) over the other two Mo–O bonds (average 2.023, 2.018 Å). These structures conform well to the general rules given elsewhere for dioxomolybdenum complexes.[10] Figures 3 and 5 show this general molybdenum environment from two different perspectives.

The phenyl ring of the ligand in each case is normal, and there is no conjugation between it and the hydroxamic acid group. This is indicated by both the C–N bond length and the fact that the phenyl ring and the hydroxamic acid group are not coplanar. For MoO_2L_2 and $MoO_2L'_2$, respectively, the C–N bond lengths average 1.430 and 1.439 Å and these distances indicate single carbon–nitrogen bonds, in view of the sp² hybridization of nitrogen (the three bond angles about the nitrogen atoms average 120.0° for each of the two compounds).

Table II. Bond Distances and Closest Intermolecular Contacts (A)

	(a) MoO_2L_2		
Mo-O(1)	1.703 (2)	C(3A)-C(4A)	1.396 (4)
Mo-O(2)	1.703 (2)	C(4A)-C(5A)	1.385 (4)
Mo-O(1A)	2.025 (2)	C(5A)-C(6A)	1.394 (4)
Mo-O(2A)	2.199 (2)	C(7A)-C(8A)	1.488 (4)
Mo-O(1B)	2.021 (2)	C(9A)-C(10A)	1.500 (5)
Mo-O(2B)	2.191 (2)	C(1B)-C(2B)	1.380 (4)
O(1A)-N(A)	1.391 (3)	C(1B)-C(6B)	1.390 (4)
O(2A)-C(7A)	1.270 (3)	C(2B)-C(3B)	1.389 (4)
O(3A)-C(4A)	1.351 (3)	C(3B)-C(4B)	1.389 (4)
O(3A)-C(9A)	1.446 (4)	C(4B)-C(5B)	1.372 (4)
O(1B)-N(B)	1.387 (3)	C(5B)-C(6B)	1.394 (4)
O(2B)-C(7B)	1.260 (3)	C(7B)-C(8B)	1.490 (4)
O(3B)-C(4B)	1.367 (4)	C(9B)-C(10B)	1.492 (5)
O(3B)-C(9B)	1.433 (4)	⟨C-H⟩	0.96
N(A)-C(1A)	1.440 (4)		
N(A)-C(7A)	1.303 (4)	O(1)-C(7B)	3.032 (4)[a]
N(B)-C(1B)	1.420 (4)	O(1)-O(2)	3.174 (3)[a]
N(B)-C(7B)	1.318 (4)	O(2)-C(7A)	2.944 (4)[b]
C(1A)-C(2A)	1.363 (4)	O(2)-N(A)	3.160 (3)[b]
C(1A)-C(6A)	1.386 (4)		
C(2A)-C(3A)	1.400 (4)		
	(b) $MoO_2L'_2$		
Mo-O(1)	1.704 (3)	C(4A)-C(5A)	1.381 (9)
Mo-O(2)	1.692 (3)	C(5A)-C(6A)	1.364 (8)
Mo-O(1A)	2.025 (3)	C(7A)-C(8A)	1.486 (7)
Mo-O(2A)	2.195 (3)	C(1B)-C(2B)	1.369 (6)
Mo-O(1B)	2.011 (3)	C(1B)-C(6B)	1.360 (6)
Mo-O(2B)	2.206 (3)	C(2B)-C(3B)	1.405 (8)
O(1A)-N(A)	1.384 (4)	C(3B)-C(4B)	1.334 (8)
O(2A)-C(7A)	1.263 (5)	C(4B)-C(5B)	1.382 (7)
O(1B)-N(B)	1.388 (4)	C(5B)-C(6B)	1.389 (7)
O(2B)-C(7B)	1.264 (5)	C(7B)-C(8B)	1.480 (6)
N(A)-C(1A)	1.430 (6)	⟨C-H⟩	0.92
N(A)-C(7A)	1.311 (5)		
N(B)-C(1B)	1.447 (6)	O(1)-C(7B)	3.213 (6)[c]
N(B)-C(7B)	1.308 (5)	O(1)-C(8B)	3.285 (6)[c]
C(1A)-C(2A)	1.377 (7)	O(2)-C(4B)	3.133 (6)[d]
C(1A)-C(6A)	1.371 (6)	O(2)-C(8A)	3.168 (7)[e]
C(2A)-C(3A)	1.376 (8)		
C(3A)-C(4A)	1.370 (9)		

[a] $x, 1/2 - y, z - 1/2$. [b] $x, 1/2 - y, 1/2 + z$. [c] $1/2 - x, y - 1/2, z$. [d] $1/2 + x, y, -z - 1/2$. [e] $1/2 - x, 1/2 + y, z$.

Table III. Bond Angles (Deg)

(a) MoO_2L_2

O(1)-Mo-O(2)	103.94 (11)	N(A)-C(1A)-C(6A)	119.2 (3)
O(1)-Mo-O(1A)	107.52 (9)	C(2A)-C(1A)-C(6A)	121.3 (3)
O(1)-Mo-O(2A)	90.15 (10)	C(1A)-C(2A)-C(3A)	120.4 (3)
O(1)-Mo-O(1B)	87.94 (9)	C(2A)-C(3A)-C(4A)	119.0 (3)
O(1)-Mo-O(2B)	158.87 (9)	C(3A)-C(4A)-C(5A)	119.7 (3)
O(2)-Mo-O(1A)	87.49 (9)	O(3A)-C(4A)-C(3A)	124.4 (3)
O(2)-Mo-O(2A)	158.91 (9)	O(3A)-C(4A)-C(5A)	115.9 (3)
O(2)-Mo-O(1B)	105.69 (9)	C(4A)-C(5A)-C(6A)	120.9 (3)
O(2)-Mo-O(2B)	90.82 (9)	C(1A)-C(6A)-C(5A)	118.6 (3)
O(1A)-Mo-O(2A)	73.16 (7)	O(2A)-C(7A)-N(A)	117.7 (3)
O(1A)-Mo-O(1B)	156.93 (9)	O(2A)-C(7A)-C(8A)	121.5 (3)
O(1A)-Mo-O(2B)	87.87 (8)	N(A)-C(7A)-C(8A)	120.9 (3)
O(2A)-Mo-O(1B)	90.20 (8)	O(3A)-C(9A)-C(10A)	108.2 (3)
O(2A)-Mo-O(2B)	80.36 (8)	N(B)-C(1B)-C(2B)	120.1 (3)
O(1B)-Mo-O(2B)	73.37 (7)	N(B)-C(1B)-C(6B)	120.2 (3)
Mo-O(1A)-N(A)	116.8 (2)	C(2B)-C(1B)-C(6B)	119.6 (3)
Mo-O(2A)-C(7A)	114.7 (2)	C(1B)-C(2B)-C(3B)	119.5 (3)
C(4A)-O(3A)-C(9A)	118.5 (2)	C(2B)-C(3B)-C(4B)	120.4 (3)
Mo-O(1B)-N(B)	116.5 (2)	C(3B)-C(4B)-C(5B)	120.4 (3)
Mo-O(2B)-C(7B)	114.3 (2)	O(3B)-C(4B)-C(3B)	115.4 (3)
C(4B)-O(3B)-C(9B)	118.0 (3)	O(3B)-C(4B)-C(5B)	124.2 (3)
O(1A)-N(A)-C(1A)	113.4 (2)	C(4B)-C(5B)-C(6B)	119.0 (3)
O(1A)-N(A)-C(7A)	116.7 (2)	C(1B)-C(6B)-C(5B)	120.8 (3)
C(1A)-N(A)-C(7A)	129.7 (3)	O(2B)-C(7B)-N(B)	118.2 (3)
O(1B)-N(B)-C(1B)	115.6 (2)	O(2B)-C(7B)-C(8B)	121.3 (3)
O(1B)-N(B)-C(7B)	115.7 (2)	N(B)-C(7B)-C(8B)	120.5 (3)
C(1B)-N(B)-C(7B)	128.7 (3)	O(3B)-C(9B)-C(10B)	108.3 (3)
N(A)-C(1A)-C(2A)	119.5 (3)		

(b) $MoO_2L'_2$

O(1)-Mo-O(2)	105.2 (2)	C(1B)-N(B)-C(7B)	128.6 (4)
O(1)-Mo-O(1A)	105.8 (2)	N(A)-C(1A)-C(2A)	119.8 (5)
O(1)-Mo-O(2A)	89.6 (2)	N(A)-C(1A)-C(6A)	120.6 (4)
O(1)-Mo-O(1B)	88.3 (1)	C(2A)-C(1A)-C(6A)	119.6 (5)
O(1)-Mo-O(2B)	159.0 (2)	C(1A)-C(2A)-C(3A)	119.8 (6)
O(2)-Mo-O(1A)	86.9 (1)	C(2A)-C(3A)-C(4A)	120.6 (6)
O(2)-Mo-O(2A)	157.9 (2)	C(3A)-C(4A)-C(5A)	119.1 (6)
O(2)-Mo-O(1B)	107.6 (2)	C(4A)-C(5A)-C(6A)	120.5 (6)
O(2)-Mo-O(2B)	90.0 (2)	C(1A)-C(6A)-C(5A)	120.4 (5)
O(1A)-Mo-O(2A)	73.1 (1)	O(2A)-C(7A)-N(A)	117.6 (4)
O(1A)-Mo-O(1B)	156.7 (1)	O(2A)-C(7A)-C(8A)	121.8 (5)
O(1A)-Mo-O(2B)	89.3 (1)	N(A)-C(7A)-C(8A)	120.6 (5)
O(2A)-Mo-O(1B)	88.9 (1)	N(B)-C(1B)-C(2B)	119.4 (4)
O(2A)-Mo-O(2B)	80.7 (1)	N(B)-C(1B)-C(6B)	118.6 (4)
O(1B)-Mo-O(2B)	73.1 (1)	C(2B)-C(1B)-C(6B)	122.1 (5)
Mo-O(1A)-N(A)	116.9 (3)	C(1B)-C(2B)-C(3B)	117.5 (5)
Mo-O(2A)-C(7A)	115.1 (3)	C(2B)-C(3B)-C(4B)	121.2 (5)
Mo-O(1B)-N(B)	117.2 (2)	C(3B)-C(4B)-C(5B)	120.6 (5)
Mo-O(2B)-C(7B)	115.0 (3)	C(4B)-C(5B)-C(6B)	119.3 (5)
O(1A)-N(A)-C(1A)	114.4 (4)	C(1B)-C(6B)-C(5B)	119.3 (5)
O(1A)-N(A)-C(7A)	116.5 (4)	O(2B)-C(7B)-N(B)	117.1 (4)
C(1A)-N(A)-C(7A)	128.9 (4)	O(2B)-C(7B)-C(8B)	122.4 (4)
O(1B)-N(B)-C(1B)	114.5 (3)	N(B)-C(7B)-C(8B)	120.5 (4)
O(1B)-N(B)-C(7B)	116.9 (4)		

The angles between the *N*-phenyl rings and the hydroxamic acid groups are 80.8 and 79.9° for MoO_2L_2 and 89.4 and 85.1° for $MoO_2L'_2$ (Table IV). Thus the two planar groups are approximately orthogonal in each ligand, prohibiting the π-orbital overlap required for conjugative interaction. The actual angles between the planar groups are influenced by crystal packing forces, which differ for the two crystal lattices and result in the different values observed for the two complexes.

The complexes derived from phenacetin, acetanilide, *p*-chloroacetanilide, *p*-(benzyloxy)acetanilide, and benzanilide each exhibited a carbonyl stretch at 1550 cm^{-1} and *cis*-dioxo frequencies at 950 and 920 cm^{-1}. The NMR spectrum of the dioxo complex of phenacetin had the following features: 7.6–7.0 ppm, quartet (4 protons, phenyl ring); 4.0 ppm, quartet (2 protons, OCH_2CH_3); 2.0 ppm, singlet (3 protons, CH_3CO); 1.3 ppm, triplet (3 protons, OCH_2CH_3). The *p*-chloroacetanilide complex has essentially the same spectrum with the ethoxy peaks absent: 7.6–7.0 ppm, quartet (4 protons); 2.1 ppm (singlet, 3 protons). Similar spectra are observed for the other complexes, as follows. Acetanilide: 7.6–7.0 ppm, multiplet (5 protons, phenyl); 2.1 ppm, singlet (3 protons). *p*-(Benzyloxy)acetanilide: 7.6–7.0 ppm, quartet (4 protons, phenyl); 7.2 ppm, singlet (5 protons, phenyl); 4.5 ppm, singlet (2 protons, $CH_2C_6H_5$); 2.1 ppm, singlet (3 protons, CH_3CO). Benzanilide: 7.3 ppm, broad singlet (phenyls). The strong spectral similarities indicate that all the dioxo complexes are likely to have similar structures.

Conclusion

Thus we report a synthesis of molybdenum hydroxamates, which could serve as a convenient source of hydroxamic acids for biochemical and pharmacological studies. The hydroxamates are stable indefinitely when complexed to molybdenum in this manner. This presents a useful method for the storage of the reactive hydroxamic acids. Studies that in the past were hampered by availability of the hydroxamic acids may find some use of this procedure. Furthermore the first direct structural information on the alleged toxic metabolite of phenacetin is reported herein. The generality of this process was demonstrated with other amides.

Acknowledgment. Support received under NSF Grant CHE77-01372 is gratefully acknowledged.

Registry No. MoO_2L_2 (R = OC_2H_5, R′ = CH_3), 76514-85-7; MoO_2L_2 (R = H, R′ = CH_3), 76581-99-2; MoO_2L_2 (R = Cl, R′ = CH_3), 76514-86-8; MoO_2L_2 (R = $OC(O)C_6H_5$, R′ = CH_3), 76514-87-9; MoO_2L_2 (R = H, R′ = C_6H_5), 76582-00-8; phenacetin, 62-44-2; acetanilide, 103-84-4; *p*-chloroacetanilide, 539-03-7; *p*-(benzoyloxy)acetanilide, 537-52-0; benzanilide, 93-98-1; MoO_3HMPT, 25377-12-2; BSA, 10416-58-7.

Supplementary Material Available: Tables of least-squares planes and observed and calculated structure factors (21 pages). Ordering information is given on any current masthead page.

Contribution from the Anorganisch Chemisch Laboratorium and the Laboratorium voor Kristallografie, University of Amsterdam, J. H. van't Hoff Instituut, 1018 WV Amsterdam, The Netherlands

Binuclear Metal Carbonyl DAB Complexes. 9. Syntheses and X-ray Structure of (μ-Acetylene)-[σ-N,σ-N′,η^2-C=N,η^2-C=N′-glyoxal bis(isopropylimine)]tetracarbonyldiruthenium. First Example of the 8e-Donating DAB Ligand (DAB = 1,4-Diazabutadiene)

L. H. STAAL, G. VAN KOTEN, K. VRIEZE,* F. PLOEGER, and C. H. STAM

Received September 16, 1980

The reactions between $Ru_2(CO)_6$[glyoxal bis(isopropylimine)] or $Ru_2(CO)_6$[glyoxal bis(cyclohexylimine)] and acetylene (HC≡CH) yield complexes of the composition $Ru_2(CO)_4$(DAB)(HC≡CH). A crystal structure determination has been carried out for (μ-acetylene)[$\sigma,\sigma,\eta^2,\eta^2$-glyoxal bis(isopropylimine)]tetracarbonyldiruthenium. The crystals are orthorhombic, of space groups $P2_12_12_1$, with four molecules in a unit cell of dimensions a = 9.541 (1), b = 13.054 (1), and c = 13.404 (1) Å. The structure was solved by means of the heavy-atom method and refined to R = 0.034 for 1600 reflections. The binuclear metal carbonyl fragment contains a two-electron Ru–Ru bond of length 2.936 (1) Å. The metal–metal bond is bridged by a DAB molecule which is coordinated to one of the ruthenium atoms via the lone pairs of the N atoms and to the other ruthenium atom via the π electrons of the two C–N double bonds. This is the first example of a σ-N,σ-N′,η^2-C=N,η^2-C=N′-coordinated 1,4-diazabutadiene ligand. The Ru–Ru bond is furthermore bridged by an acetylene forming in Ru–C σ bonds of lengths 2.09 and 2.06 Å. The coordinated acetylene is parallel to the Ru–Ru bond. The ^{1}H NMR chemical shifts for the imine hydrogen atoms are observed near 6.2 ppm, which is in agreement with the proposed bonding mode for the DAB ligand.

Introduction

Studies of the coordination behavior of 1,4-diazabutadienes (DAB = R_1N=$C(R_2)(R_2)C$=NR_1) revealed an interesting variety of bonding modes for this heterobutadiene molecule. In principle a maximum of eight electrons are available for coordination: two lone pairs on the imine nitrogen atoms and two pairs of π electrons on the N=C—C=N skeleton.

The predominant cooridnation mode is chelate ring formation via the two lone pairs on nitrogen,[1-8] but recently the σ-N monodentate and σ-N,σ-N′ bridging modes have also been established.[9,10]

Involvement of the π electrons of the N=C—C=N skeleton in the coordination toward methyl carbonyl complexes has been the subject of extensive investigations. A series of binuclear metal carbonyl complexes of the general formula $MM'(CO)_6$(DAB) has been synthesized (M = M′ = Fe,[11] Ru,[12,13] Os;[14] M = Co and M′ = Mn, Re.[15] In all these complexes the DAB ligand is coordinated via the two lone pairs on nitrogen and via one pair of π electrons, thus being a six-electron donating system. Only one example is known at present of a complex containing two DAB ligands coordinated in the 6e donor mode: $Ru_2(CO)_4(DAB)_2$.[13]

Although the N=C—C=N system might be regarded as a formal analogue of butadiene, the π,π-bonding mode which is commonly found for the butadienes has so far not been observed for 1,4-diazabutadienes. We now report the first example of the σ-N,σ-N′,η^2-C=N,η^2-C=N′ coordination mode of 1,4-diazabutadienes. In addition to the two lone pairs on nitrogen, the ligand uses both pairs of π electrons of the N=C—C=N skeleton for the coordination toward a binuclear ruthenium fragment.

Experimental Section

^{1}H NMR spectra were recorded with a Varian T 60 and a Varian XL 100 apparatus, IR spectra were obtained with a Perkin-Elmer 283 spectrophotometer, and mass spectra have been recorded with a Varian MAT 711 mass spectrometer, using a field desorption device. The elemental analyses were carried out by the Section Elemental Analysis of the Institute for Organic Chemistry, TNO, Utrecht, The Netherlands.

$Ru_3(CO)_{12}$ and acetylene were obtained from commercial sources

*To whom correspondence should be addressed at the Anorganisch Chemisch Laboratorium.

(1) Staal, L. H.; Stufkens, D. J.; Oskam, A. *Inorg. Chim. Acta* **1978**, *26*, 255.
(2) Staal, L. H.; van Koten, G.; Vrieze, K. *J. Organomet. Chem.* **1979**, *175*, 73.
(3) Staal, L. H.; Polm, L. H.; Vrieze, K. *Inorg. Chim. Acta* **1980**, *40*, 165.
(4) Klerks, J. M.; Stufkens, D. J.; van Koten, G.; Vrieze, K. *J. Organomet. Chem.* **1979**, *181*, 271.
(5) Frühauf, H. W.; Grevels, F. W.; Landers, A. *J. Organomet. Chem.* **1979**, *178*, 349.
(6) Grociani, B.; Bandoli, G.; Clemente, D. A. *J. Organomet. Chem.* **1980**, *190*, C97 and references therein.
(7) Svoboda, M.; tom Dieck, H. *J. Organomet. Chem.* **1980**, *191*, 321.
(8) Bock, H.; tom Dieck, H. *Chem. Ber.* **1967**, *100*, 228.
(9) van der Poel, H.; van Koten, G.; Vrieze, K.; Kokkes, M.; Stam, C. H. *J. Organomet. Chem.* **1979**, *175*, C21.
(10) van der Poel, H.; van Koten, G.; Vrieze, K.; Kokkes, M.; Stam. C. H. *Inorg. Chim. Acta* **1980**, *39*, 197.
(11) Frühauf, H. W.; Landers, A.; Goddard, R.; Krüger, C. *Angew. Chem.* **1978**, *90*, 56.
(12) Staal, L. H.; Polm, L. H.; van Koten, G.; Vrieze, K. *Inorg. Chim. Acta* **1979**, *37*, L485.
(13) Staal, L. H.; Polm, L. H.; Balk, R. W.; van Koten, G.; Vrieze, K.; Brouwers, A. M. F. *Inorg. Chem.* **1980**, *19*, 3343.
(14) Staal, L. H.; van Koten, G.; Vrieze, K. *J. Organomet. Chem.*, in press.
(15) Staal, L. H.; Keijsper, J.; van Koten, G.; Vrieze, K.; Cras, J. A.; Bosman, W. *Inorg. Chem.* **1981**, *20*, 555.

0020-1669/81/1320-1830$01.25/0